International Journal of Thermophysics, Vol. 20, No. 6, 1999

An Equation of State for 1,1,1-Trifluoroethane (R-143a)[1]

J. Li,[2-4] R. Tillner-Roth,[5] H. Sato,[2] and K. Watanabe[2]

A fundamental equation of state has been developed for 1,1,1-trifluoroethane (R-143a) using the dimensionless Helmholtz energy. The experimental thermodynamic property data, which cover temperatures from the triple point (161 K) to 433 K and pressures up to 35 MPa, are used to develop the present equation. These data are represented by the present equation within their reported experimental uncertainties: ±0.1% in density for both vapor and liquid phase P-ρ-T data, ±1% in isochoric specific heat capacities, and ±0.02% in the vapor phase speed-of-sound data. The extended range of validity of the present model covers temperatures from 160 to 650 K and pressures up to 50 MPa as verified by the thermodynamic behavior of the isobaric heat-capacity values over the entire fluid phase.

KEY WORDS: alternative refrigerant; equation of state; Helmholtz energy; R-143a; 1,1,1-trifluoroethane.

1. INTRODUCTION

Binary and ternary refrigerant mixtures containing 1,1,1-trifluoroethane (R-143a) are the most promising candidates to replace the conventional azeotropic refrigerant R-502 currently being used exclusively for low-temperature refrigeration systems. The equation of state for R-143a is needed not only to represent the thermodynamic properties for the pure fluid, but

---

[1] Paper presented at the Thirteenth Symposium on Thermophysical Properties, June 22-27, 1997, Boulder, Colorado, U.S.A.

[2] Department of System Design Engineering, Faculty of Science and Technology, Keio University, 3-14-1 Hiyoshi, Kohoku-ku, Yokohama 223-8522, Japan.

[3] Present address: Technology Center, Changhong Electronic Group Corporation, High Technology Zone, Mianyang City, Sichuan 621000, P.R. China.

[4] To whom correspondence should be addressed.

[5] Institute of Thermodynamics, University of Hannover, Callinstrasse 36, D-30167 Hannover, Germany.

also as a basic equation to develop a thermodynamic model for refrigerant mixtures containing R-143a. Like other HFC refrigerants considered as substitutes for CFCs and HCFCs, the thermodynamic properties of R-143a have been investigated rather extensively in recent years. Available experimental data include 1063 points of P–ρ–T data in the vapor phase, 1779 points in the liquid phase, 642 points of thermodynamic property data along the coexistence curve, and 922 points of caloric property data. The temperature and pressure ranges of the experimental thermodynamic properties are wide enough, and the uncertainties of those data are reliable enough, to develop a so-called wide-range equation of state.

In this paper, an equation of state explicit in the dimensionless Helmholtz energy is presented. A regression analysis developed by Wagner [1] was used to find the suitable structure of the equation with respect to the linear data, while a nonlinear optimization method proposed by Ahrendts and Baehr [2] was adopted to modify the equation on the basis of available thermodynamic property data, especially isobaric heat capacity and speed-of-sound data. All of the equations and the temperature values in this paper are given on the International Temperature Scale of 1990 (ITS-90).

2. EXPERIMENTAL DATA

Not all of the existing thermodynamic property data were selected as input data to develop the present equation of state. The selection was done on the basis of an analysis of the experimental uncertainties reported, the magnitude of their scatter, and the thermodynamic consistency with other data sets.

The observed critical temperature and density values by Aoyama et al. [3], $T_c = 345.86 \pm 0.01$ K and $\rho_c = 434 \pm 1$ kg $\cdot$ m^{-3}, were selected as the numerical constants, i.e., T^* $(=T_c)$ and ρ^* $(=\rho_c)$, to define the reduced density δ $(=\rho/\rho^*)$ and inverse reduced temperature τ $(=T^*/T)$, which were used as the independent variables in the present modeling.

Eight points of the ideal-gas isobaric specific heat-capacity values, C_p^0, by Gillis [4] were used to establish a C_p^0 correlation for the ideal-gas state. These data were derived from speed-of-sound measurements for temperatures from 250 to 400 K. Taking into account the contributions of anharmonicities, Yokozeki et al. [5] recalculated the ideal gas isobaric specific heat-capacity values based on the spectroscopic data. The calculated results between 160 K (the triple-point temperature) and 700 K were also selected as additional input data in the present study.

Five hundred thirty-six vapor-phase P–ρ–T data of de Vries [6], which cover the range of temperatures 263 to 433 K and pressures 0.02 to

20.6 MPa, were selected as the basic data for the vapor phase. In the liquid phase, 526 P–ρ–T data of de Vries were used, which cover the range of 243 to 393 K and 1.48 to 18.1 MPa. In addition, 102 P–ρ–T data of Magee [7] beyond the range in which de Vries' data exist were used.

The vapor-pressure data observed by deVries [6] were selected to represent the thermodynamic properties at saturation. The measurements by Russel et al. [8] were also added so as to represent the behavior at lower temperatures where no other data exist. The input data thus selected from deVries and from Russel et al. cover the temperature range of 173 to 345 K.

One hundred thirty-six isochoric specific heat-capacity data in the liquid phase, as well as those at the saturated-liquid condition from the triple point to the critical temperature, reported by Magee [7] were also selected as the input data. Eighty-six speed-of-sound measurements in the vapor phase by Gillis [4] were also included.

3. EQUATION OF STATE

The developed equation of state for R-143a, given in the dimensionless Helmholtz energy, $\Phi(\tau, \delta)$, is split into two parts: an ideal part, Φ^0, which describes the ideal-gas behavior, and a residual part, Φ^r, which is responsible for the representation of thermodynamic behavior of the real fluid, as given below:

$$\Phi(\tau, \delta) = \frac{A}{RT} = \Phi^0(\tau, \delta) + \Phi^r(\tau, \delta) \tag{1}$$

where A is the specific Helmholtz energy, $R = R_m/M$ is the gas constant of R-143a using the universal gas constant $R_m = 8.31451\ \mathrm{J \cdot mol^{-1} \cdot K^{-1}}$, and $M = 0.084041\ \mathrm{kg \cdot mol^{-1}}$ is the molar mass. The parameters τ and δ are the independent variables mentioned previously.

The ideal part, $\Phi^0(\tau, \delta)$, of the equation of state is given by

$$\Phi^0(\tau, \delta) = \ln(\delta) + a_1^0 + a_2^0\tau + a_3^0 \ln(\tau) + a_4^0\tau^{-3/2} + a_5^0\tau^{5/4} + a_6^0\tau^{-1} \tag{2}$$

The first term comes from the ideal-gas law, i.e., $P = \rho RT$. The next two constants a_1^0 and a_2^0 in Eq. (2) were adjusted so that the saturated liquid enthalpy and entropy values calculated from Eq. (1) at 273.15 K are $200\ \mathrm{kJ \cdot kg^{-1}}$ and $1\ \mathrm{kJ \cdot kg^{-1} \cdot K^{-1}}$, respectively. These two numerical constants were determined after developing the residual part of the equation of state. The last four terms on the right-hand side of Eq. (2) are related to an empirical correlation of the ideal-gas isobaric specific heat capacity,

$C_p^0(T)$. Initially, Eq. (2) was developed based on the selected C_p^0 data. Later, the coefficients of a_3^0, a_4^0, a_5^0, and a_6^0 were slightly readjusted simultaneously with the optimization of the residual part Φ^{r} in order to take into account the caloric property behavior of the real fluid in the vapor phase. The final values of these coefficients thus determined are

$$a_1^0 = -0.5556942 \times 10, \qquad a_2^0 = 0.8937480 \times 10, \qquad a_3^0 = -0.8999794$$

$$a_4^0 = 0.1652398 \times 10, \qquad a_5^0 = -0.6827433, \qquad a_6^0 = -0.8113464 \times 10$$

Equation (2) is valid for temperatures from 100 to 700 K.

Two optimization strategies have been employed to develop the residual part $\Phi^{\mathrm{r}}(\tau, \delta)$ of the present model. The first one consists of the regression analysis developed by Wagner [1], in which essential terms of significant importance are selected from a bank with a large number of terms. For R-143a, such an initial bank of terms is given by the following expression:

$$\Phi^{\mathrm{r}}(\tau, \delta) = \sum_i a_i \delta^{d_i} \tau^{t_i} + \sum_i a_i \delta^{d_i} \tau^{t_i} e^{-\delta^{c_i}} \tag{3}$$

It consists of polynomial terms of δ and τ and supplementary terms associated with an exponential function, $\exp(-\delta^{c_i})$, where the exponent c_i varies from 1 to 4. About 500 terms are taken into consideration regarding the bank of terms given by Eq. (3).

The linear data such as P–ρ–T properties and isochoric specific heat capacities were used to find a suitable structure for the residual part $\Phi^{\mathrm{r}}(\tau, \delta)$. Besides the linear experimental thermodynamic properties, two additional constraints were also included in the present regression analysis.

(a) Thermodynamic constraints at the critical point:

$$(\partial p/\partial \rho)_{T|_{\rho=\rho_c}^{T=T_c}} = 0, \qquad (\partial^2 p/\partial \rho^2)_{T|_{\rho=\rho_c}^{T=T_c}} = 0 \tag{4}$$

(b) The Maxwell relation regarding the saturation properties at a given temperature:

$$\Phi^{\mathrm{r}}(\tau, \delta') - \Phi^{\mathrm{r}}(\tau, \delta'') = \frac{P_{\mathrm{s}}}{RT}\left(\frac{1}{\rho''} - \frac{1}{\rho'}\right) - \ln \frac{\rho'}{\rho''} \tag{5}$$

where P_{s} denotes the saturation pressure and ρ' and ρ'' are the saturated liquid and vapor densities, respectively.

The method proposed in Ref. 2 was used for the nonlinear optimization as a next step to readjust the coefficients of the equation of state based on all of the selected linear and nonlinear experimental thermodynamic

Table I. Numerical Constants in Eq. (6)

i	a_i	c_i	t_i	d_i
1	0.1606645×10^{-1}	–	0	5
2	0.4163515×10		0.5	1
3	-0.5031058×10		0.75	1
4	$-0.1920208 \times 10^{-1}$		2.5	2
5	0.1470093×10^{-2}		2.5	4
6	0.1775429	1	0.25	3
7	$-0.7316069 \times 10^{-2}$	1	0.25	8
8	$-0.9555916 \times 10^{-1}$	1	2	3
9	-0.5822518	1	3	1
10	$-0.4211022 \times 10^{-3}$	2	3	10
11	$-0.2059847 \times 10^{-1}$	2	8	1
12	0.3711325×10^{-1}	2	8	4
13	0.1799723×10^{-3}	2	8	8
14	$-0.4145922 \times 10^{-1}$	2	10	2
15	0.7682566×10^{-4}	3	8	12
16	$-0.2089695 \times 10^{-2}$	3	17	8
17	0.1958633×10^{-2}	3	20	2
18	$-0.3198325 \times 10^{-5}$	3	35	5
19	$-0.5376561 \times 10^{-2}$	4	27	3

property data such as speed of sound and isochoric heat capacity. The final form of the residual part $\Phi^{\mathrm{r}}(\tau, \delta)$ developed in the present study is

$$\Phi^{\mathrm{r}}(\tau, \delta) = \sum_{i=1}^{5} a_i \delta^{d_i} \tau^{t_i} + \sum_{i=6}^{19} a_i \delta^{d_i} \tau^{t_i} e^{-\delta^{c_i}} \tag{6}$$

The numerical coefficients of a_i and exponents d_i, t_i, and c_i are listed in Table I.

4. RESULTS AND DISCUSSION

The critical parameter values calculated from the present equation of state are $T_c = 345.86$ K, $P_c = 3.764$ MPa, and $\rho_c = 434$ kg · m^{-3}. The critical temperature T_c and critical density ρ_c agree with the measurements by Aoyama et al. [3]. The critical pressure calculated from the present equation differs slightly from most of the reported values within ± 5 kPa, which is smaller than the uncertainty reported for the critical pressure values.

Triple-point temperature measurements are reported by Magee [7] and Russel et al. [8], although no triple-point pressure or density data are reported. The triple-point pressure estimated by Tillner-Roth [9] is 1.091 kPa, corresponding to the triple-point temperature $T_{\mathrm{t}} = 161.34$ K

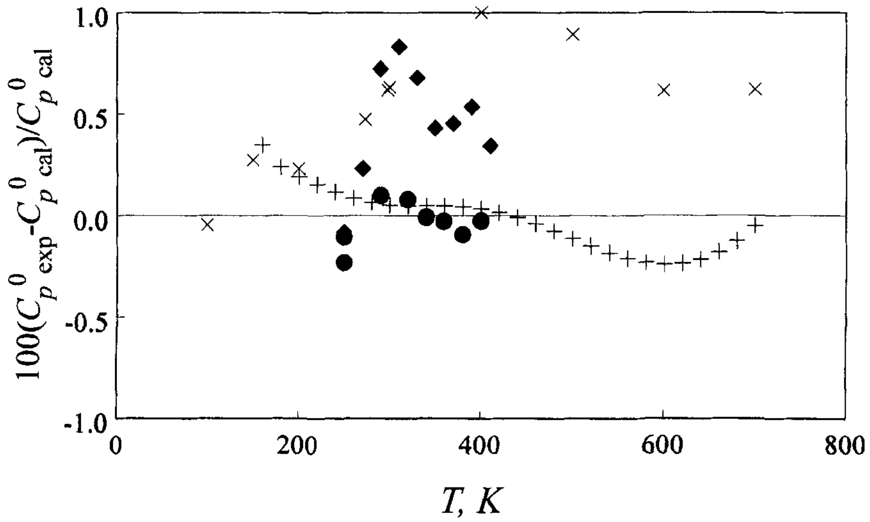

Fig. 1. Deviations of ideal gas isobaric specific heat-capacity values from the present equation: (●) Gillis [4]; (◆) Beckermann and Kohler [10]; (×) Chen et al. [11]; (+) Yokozeki et al. [5].

measured by Magee. At the same triple-point temperature, the present model yields $T_t = 161.34$ K, $\rho'_t = 1329\ \mathrm{kg \cdot m^{-3}}$, $\rho''_t = 0.068\ \mathrm{kg \cdot m^{-3}}$, and $p_t = 1.080$ kPa, which differs from the value by Tillner-Roth [9] by only 11 Pa.

Figure 1 shows the deviations of the reported ideal gas isobaric specific heat-capacity values from the present equation. The data of Gillis [4] are well represented by Eq. (1) within ±0.3%, whereas the results of Beckermann and Kohler [10] show a larger scatter of up to ±1%. Theoretical values by Chen et al. [11] are represented within ±1% for temperatures from 100 to 700 K, while the values of Yokozeki et al. [5], which include anharmonicity corrections, are well represented within ±0.4% for temperatures from 160 to 700 K.

For an easy comparison of the P-ρ-T properties, we divide the entire fluid phase into the following four regions since the quantity of data is too large.

Vapor-phase region: $T \leqslant 344$ K, $P < P_s$ or $T > 344$ K, $\rho \leqslant 250\ \mathrm{kg \cdot m^{-3}}$
Liquid-phase region: $T \leqslant 344$ K, $P > P_s$ or $T > 344$ K, $\rho \geqslant 650\ \mathrm{kg \cdot m^{-3}}$
Near-critical region: $344\ \mathrm{K} < T \leqslant 353$ K and
$250\ \mathrm{kg \cdot m^{-3}} < \rho < 650\ \mathrm{kg \cdot m^{-3}}$
Supercritical region: $T > 353$ K and $250\ \mathrm{kg \cdot m^{-3}} < \rho < 650\ \mathrm{kg \cdot m^{-3}}$

Figure 2 shows the relative pressure deviations of measurements by de Vries [6] in the vapor-phase region at different pressures. Most of the measurements are well represented by the present model within ±0.05%. The lowest three isothermal Burnett measurements, which show a slightly different behavior from other measurements, are represented within ±0.1%. Several data in the liquid-phase region from the vibrating tube densimeter are represented within ±0.2% as shown in Fig. 2. Figure 3 shows the relative density deviations in the liquid-phase region at the different pressures. Most of the liquid-phase measurements by de Vries [6] are satisfactorily represented within ±0.05% except several points near the saturation boundary, which have a larger scatter of up to ±0.1%. The liquid-phase P–ρ–T measurements by Magee [7] show a slightly higher positive deviation, but all of them are represented within ±0.2%. Measurements of deVries in the near-critical region and supercritical region are represented within ±0.4% in pressure.

Figure 4 illustrates the vapor-pressure deviations with respect to temperature. The experimental vapor-pressure data of de Vries [6] are represented within ±0.035%, while those of Russel et al. [8] are represented with deviations not more than ±50 Pa. Figure 5 shows the deviations of isochoric heat-capacity data by Magee [7] in the liquid phase, where the

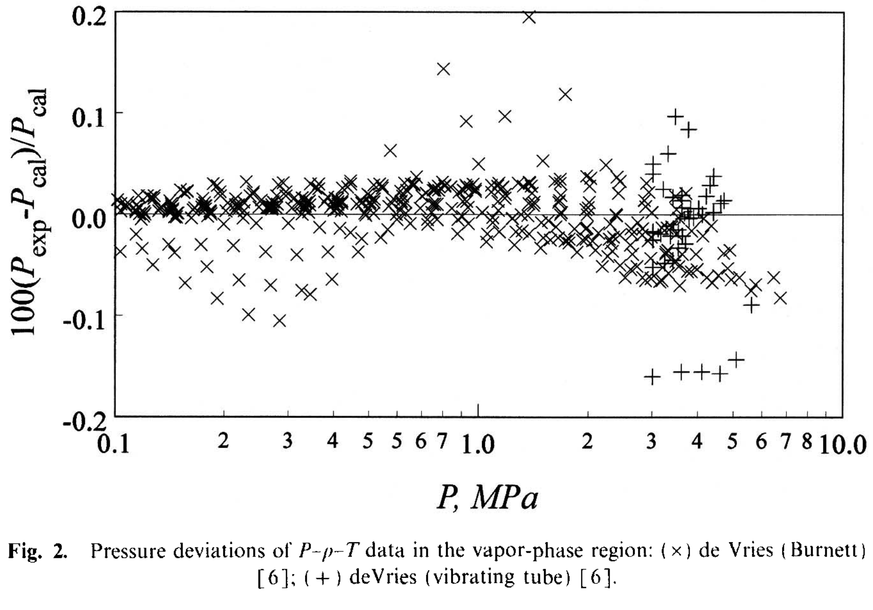

Fig. 2. Pressure deviations of P–ρ–T data in the vapor-phase region: (×) de Vries (Burnett) [6]; (+) deVries (vibrating tube) [6].

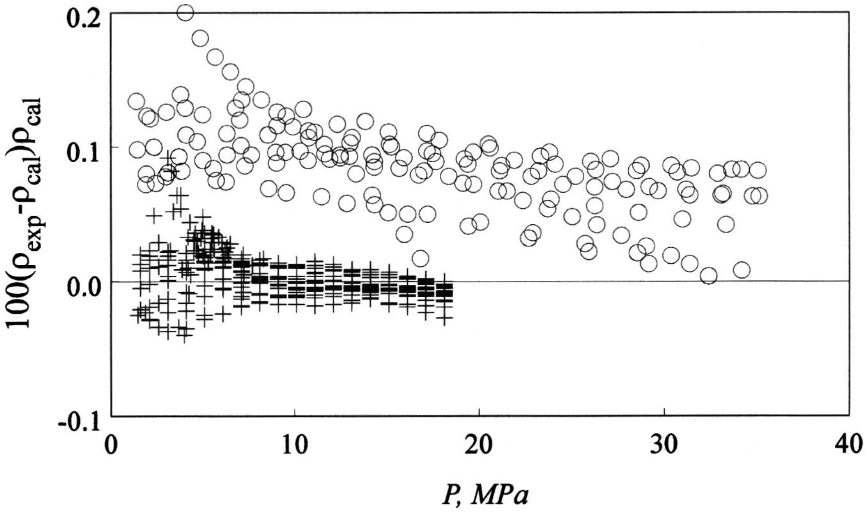

Fig. 3. Density deviations of P–ρ–T data in the liquid-phase region: (+) de Vries [6]; (○) Magee [7].

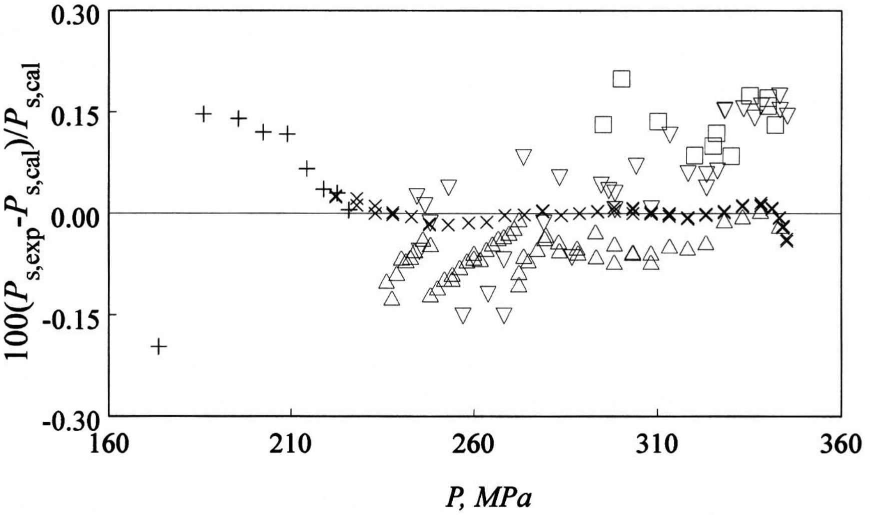

Fig. 4. Vapor-pressure deviations from the present equation: (×) de Vries [6]; (+) Russel et al. [8]; (△) Weber and Defibaugh [18]; (▽) Giuliani et al. [13]; (□) Zhang et al. [20].

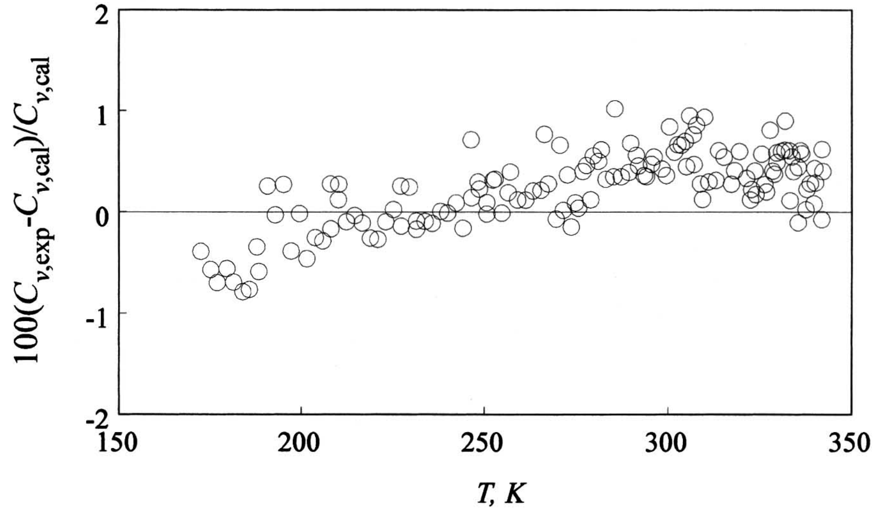

Fig. 5. Deviations of isochoric specific heat-capacities in liquid-phase region: (○) Magee [7].

measurements from the triple point to the critical temperature are well represented within ±1%.

Table II summarizes the results of a statistical analysis for all the thermodynamic properties available. The statistical quantities are defined by the following expressions in which X stands for an arbitrary property. The column labeled Bad in Table II indicates the number of data points for which the deviations exceed ±10%.

$$\mathrm{AAD}=\frac{1}{N}\sum_{i=1}^{N}\left|\left(\frac{X_{\mathrm{exp},i}-X_{cal,i}}{X_{cal,i}}\right)100\%\right| \tag{7}$$

$$\mathrm{BIAS}=\frac{1}{N}\sum_{i=1}^{N}\left(\frac{X_{\mathrm{exp},i}-X_{cal,i}}{X_{cal,i}}\right)100\% \tag{8}$$

$$\mathrm{RMS}=\sqrt{\frac{1}{N}\sum_{i=1}^{N}\left\{\left(\frac{X_{\mathrm{exp},i}-X_{cal,i}}{X_{cal,i}}\right)100\%\right\}^{2}} \tag{9}$$

Figure 6 illustrates the isobaric heat-capacity behavior derived from the present equation of state for the range of temperatures from the triple point to 650 K and pressures from 0.05 to 50 MPa.

Table II. Statistical Analysis of the Experimental Thermodynamic Properties

Reference	Year	Number of points	AAD	BIAS	RMS	MAXDEV	Bad[a]
$X = P$							
de Vries [6]	1997	536	0.036	0.002	0.096	1.522	2
Fujiwara and Piao [12]	1995	40	0.357	0.344	0.426	0.990	0
Giuliani et al. [13]	1994	14	0.103	0.103	0.115	0.233	0
Giuliani et al. [14]	1995	62	0.099	0.020	0.347	2.679	0
Mears et al. [15]	1955	21	1.250	−1.039	1.428	2.608	0
Takahashi et al. [16]	1999	106	0.308	0.268	0.745	5.682	0
Tsuge et al. [17]	1997	25	0.187	0.155	0.218	−0.376	0
Weber and Defibaugh [18]	1996	117	0.049	−0.015	0.065	0.117	0
Ye [19]	1994	58	0.170	−0.156	0.212	−0.900	0
Zhang et al. [20]	1995	84	0.063	0.001	0.079	0.193	0
$X = \rho$							
deVries [6]	1997	526	0.134	0.054	0.542	7.112	0
Defibaugh and Moldover [21]	1997	855	0.307	0.307	0.807	6.821	3
Fujimine et al. [22]	1997	39	0.228	−0.228	0.244	−0.555	0
Magee [7]	1996	144	0.085	0.085	0.092	0.233	0
Nakamura et al. [23]	1997	215	0.195	−0.163	0.354	−2.688	1
$X = C_p^0$							
Beckermann and Kohler [10]	1995	9	0.479	0.461	0.531	0.832	0
Chen et al. [11]	1975	10	0.541	0.533	0.610	1.008	0
Gillis [4]	1997	8	0.083	−0.037	0.106	−0.229	0
Mears et al. [15]	1955	6	1.501	−0.889	1.591	−1.880	0
Smith et al. [24]	1952	4	0.658	0.567	0.786	1.097	0
Vanderkooi and deVries [25]	1956	1	0.476	0.476	0.476	0.476	0
Yokozeki et al. [5]	1997	28	0.127	−0.019	0.153	0.349	0
$X = C_v$							
Magee [7]	1996	136	0.365	0.231	0.437	1.010	0
$X = C_p$							
Mukoyama [26]	1997	4	0.520	−0.391	0.714	−1.323	0
Yamamura et al. [27]	1997	31	1.539	1.539	1.566	1.835	0
$X = w$							
Beckermann and Kohler [10]	1995	246	0.027	−0.012	0.032	−0.079	0
Gillis [4]	1997	86	0.005	0.004	0.007	0.018	0
Ichigawa et al. [28]	1997	74	0.018	−0.018	0.019	−0.028	0
Takagi [29]	1995	188	0.473	−0.026	0.593	2.584	2
$X = B$							
Beckermann and Kohler [10]	1995	9	1.564	−1.027	1.967	−3.625	0
Bignell and Dunlop [30]	1993	3	0.659	−0.659	0.742	−1.087	0
Gillis [4]	1997	13	1.314	1.220	1.365	1.856	0
Ye [19]	1994	7	3.672	3.672	3.719	4.534	0
Zhang et al. [20]	1995	7	0.480	−0.313	0.528	−0.929	0

Table II. *(Continued)*

Reference	Year	Number of points	AAD	BIAS	RMS	MAXDEV	Bad[a]
$X = P_s$							
de Vries [6]	1997	59	0.009	−0.001	0.013	−0.041	0
Doering et al. [31]	1994	31	0.305	0.166	0.383	0.998	0
Duarte-Garza and Magee [32]	1997	15	0.239	−0.239	0.252	−0.370	0
Fujiwara and Piao [12]	1995	23	0.128	0.128	0.130	0.213	0
Fukushima [33]	1993	17	0.095	−0.024	0.167	−0.628	0
Giuliani et al. [13]	1994	61	0.096	−0.066	0.135	−0.461	0
Giuliani et al. [14]	1995	33	0.083	0.045	0.100	0.174	0
Kubota et al. [34]	1990	4	0.110	−0.039	0.116	−0.170	0
Magee [7]	1996	13	0.352	−0.352	0.353	−0.393	0
Mears et al. [15]	1955	7	0.377	0.280	0.508	1.141	0
Nagel and Bier [35]	1996	26	0.246	0.246	0.247	0.293	0
Russel et al. [8]	1944	9	0.095	0.052	0.113	−0.197	0
Takahashi et al. [16]	1990	22	0.917	0.904	1.167	2.296	0
Takashima and Higashi [36]	1995	12	0.197	−0.065	0.228	−0.400	0
Tsuge et al. [17]	1997	31	0.081	0.081	0.088	0.146	0
Wang et al. [37]	1993	30	0.103	−0.100	0.117	−0.225	0
Weber and Defibaugh [18]	1996	52	0.059	−0.059	0.066	−0.126	0
Widiatmo et al. [38]	1994	12	0.324	0.324	0.388	0.774	0
Ye [19]	1994	11	0.352	0.352	0.423	0.695	0
Zhang et al. [20]	1995	11	0.136	0.136	0.140	0.199	0
$X = \rho'$							
Aoyama et al. [3]	1996	15	0.936	0.015	1.369	3.659	5
Defibaugh and Moldover [21]	1997	20	0.239	0.239	0.346	1.326	0
Doering et al. [31]	1994	4	2.214	2.214	2.361	3.396	0
Fujimine et al. [22]	1997	14	0.345	−0.345	0.371	−0.579	0
Fukushima [33]	1993	16	1.684	−1.684	1.722	−2.157	0
Higashi and Ikeda [39]	1996	7	1.921	0.619	2.961	6.328	2
Magee [7]	1996	8	0.117	0.117	0.119	0.156	0
Mears et al. [15]	1955	6	3.566	3.566	3.567	3.699	0
Widiatmo et al. [38]	1994	17	0.555	−0.555	0.579	−1.125	0
Yokoyama and Takahashi [40]	1991	16	0.337	−0.336	0.383	−0.551	0
$X = \rho''$							
Aoyama et al. [3]	1996	20	1.061	0.540	1.373	3.400	0
Fukushima [33]	1993	12	4.768	−4.768	5.212	−5.697	1
Higashi and Ikeda [39]	1996	8	0.706	0.308	0.865	1.653	0
$C = C_{v,\,Sat.\,Liq.}$							
Magee [7]	1996	80	0.347	−0.172	1.297	−4.382	3
$X = C_{p,\,Sat.\,Liq.}$							
Russel et al. [8]	1944	11	0.109	0.016	0.136	0.320	0

[a] The number of data points for which the deviations exceed ±10%.

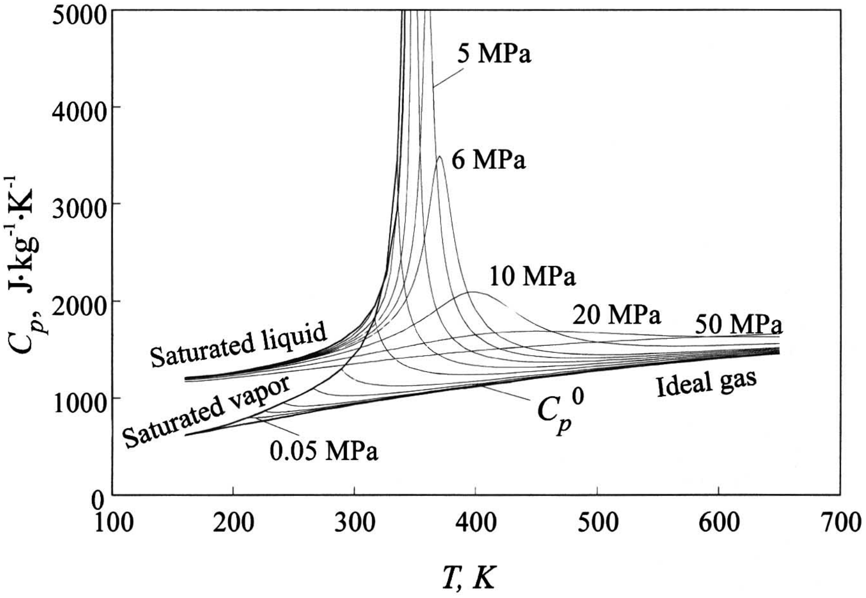

Fig. 6. Isobaric specific heat-capacity behavior derived from the present model.

ACKNOWLEDGMENTS

The authors are grateful to the NEDO (New Energy and Industrial Technology Development Organization of Japan) for financial support. We also thank all the members of the Annex 18 project at the IEA for their supply of experimental data, especially the unpublished data.

REFERENCES

1. W. Wagner, *Fortschr.-Ber. VDI-Z.* **3**(39) (1974).
2. J. Ahrendts and H. D. Baehr, *Int. Chem. Eng.* **21**:557 (1981).
3. H. Aoyama, G. Kishizawa, H. Sato, and K. Watanabe, *J. Chem. Eng. Data* **41**:1046 (1996).
4. K. A. Gillis, *Int. J. Thermophys.* **18**:73 (1997).
5. A. Yokozeki, H. Sato, and K. Watanabe, *Int. J. Thermophys.* **20**:141 (1999).
6. B. de Vries, *Thermodynamische Eigenschaften von R32, R125 und R143a*, Dissertation (University Hannover, Hannover, Germany, 1997).
7. J. W. Magee, personal communication (Natl. Inst. Stds. Tech., Boulder, CO, 1996).
8. H. Russel, D. R. V. Golding, and D. M. Yost, *J. Am. Chem. Soc.* **66**:16 (1944).
9. R. Tillner-Roth, *Int. J. Thermophys.* **17**:1365 (1996).
10. W. Beckermann and F. Kohler, *Int. J. Thermophys.* **16**:455 (1995).

11. S. S. Chen, A. S. Rodgers, J. Chao, R. C. Wilhoit, and B. J. Zwolinski, *J. Phys. Chem. Ref. Data* **4**:441 (1975).
12. K. Fujiwara and C.-C. Piao, *Proc. 16th Japan Symp. Thermophys. Prop.* (Hiroshima, Japan, 1995).
13. G. Giuliani, S. Kumar, F. Polonara, and D. Zazzini, CFC's, *The Day After, Proc. Meet. IIR Comm. B1, B2, E1, E2* (Padova, Italy, 1994).
14. G. Giuliani, S. Kumar, D. Zazzini, and F. Polonara, *J. Chem. Eng. Data* **40**:903 (1995).
15. W. H. Mears, R. F. Stahl, S. R. Orfeo, R. C. Shair, L. F. Kells, W. Thomson, and H. McCann, *Ind. Eng. Chem.* **47**:1449 (1955).
16. M. Takahashi, N. Shibasaki-Kitakawa, and C. Yokoyama, *Int. J. Thermophys.* **20**:435 (1999).
17. T. Tsuge, H. Sato, and K. Watanabe, personal communication (Keio University, Yokohama, Japan, 1997).
18. L. A. Weber and D. R. Defibaugh, *J. Chem. Eng. Data* **41**:1477 (1996).
19. F. Ye, *A Study of the Thermodynamic Properties of Pentafluoroethane (HFC-125) and 1,1,1-Trifluoroethane (HFC-143a) in the Gaseous Phase*, M.S. thesis (Keio University, Yokohama, Japan, 1994) (in Japanese).
20. H.-L. Zhang, H. Sato, and K. Watanabe, *J. Chem. Eng. Data* **40**:887 (1995).
21. D. R. Defibaugh and M. R. Moldover, *J. Chem. Eng. Data* **42**:160 (1997).
22. T. Fujimine, H. Sato, and K. Watanabe, *Int. J. Thermophys.* **20**:911 (1999).
23. S. Nakamura, K. Fujiwara, and M. Noguchi, *J. Chem. Eng. Data* **42**:334 (1997).
24. D. C. Smith, G. M. Brown, J. R. Nielsen, R. M. Smith, and C. Y. Liang, *J. Chem. Phys.* **20**:473 (1952).
25. W. N. Vanderkooi and T. de Vries, *J. Phys. Chem.* **60**:636 (1956).
26. K. Mukoyama, *Experimental Study of the Gaseous Isobaric Specific Heat Capacity for R-134a and R-143a*, M.S. thesis (Keio University, Yokohama, Japan, 1997) (in Japanese).
27. T. Yamamura, G. Yasuda, H. Sato, and K. Watanabe, submitted for publication.
28. T. Ichikawa, T. Hozumi, H. Sato, and K. Watanabe, submitted for publication.
29. T. Takagi, *Proc. 4th Asian Thermophys. Prop. Conf.* **2**:303 (1995).
30. C. M. Bignell and P. J. Dunlop, *J. Chem. Phys.* **98**:4889 (1993).
31. R. Doering, H. Buchwald, and C. Von Eynatten, *Oesterreichischer Kaelte- und Klimatechnischer Verein* (1994).
32. H. A. Duarte-Garza and J. W. Magee, *Int. J. Thermophys.* **18**:173 (1997).
33. M. Fukushima, *Trans. JAR* **10**:87 (1993).
34. H. Kubota, N. Nojiri, and T. Makita, *Rev. Phys. Chem. Japan* **1** (1990).
35. M. Nagel and K. Bier, *Int. J. Refrig.* **19**:264 (1996).
36. H. Takashima and Y. Higashi, *Proc. 16th Japan Symp. Thermophys. Prop.* (Hiroshima, Japan, 1995).
37. H. Wang, Y. Ma, C. Lu, and Y. Tian, *Beijing Gongcheng Rewuli Xuebao* **14**:122 (1993).
38. J. V. Widiatmo, H. Sato, and K. Watanabe, *J. Chem. Eng. Data* **39**:304 (1994).
39. Y. Higashi and T. Ikeda, *Fluid Phase Equil.* **125**:139 (1996).
40. C. Yokoyama and S. Takahashi, *Fluid Phase Equil.* **67**:227 (1991).